Dual-Polarized Antenna with Flexible Pattern Steering Based on Digital Meta-surface for Satellite-Assisted Mobile Communication

Guangwei Yang, *Senior Member, IEEE*, Gang Jiang, Yiwei Zhang, Yihan Ma, Lei Wang, *Senior Member, IEEE*, Zijian Xing, Dimitra Psychogiou, *Senior Member, IEEE*, and Ling Wang

***Abstract*—To address the practical challenges of satellite-assisted mobile communication for Internet-of-Things (IoT) devices—such as the needs for low-profile antennas, wide-angle beam steering under strict size and power constraints, and the limited tuning flexibility of conventional reconfigurable structures—this work proposes a compact dual-polarized antenna with digitally controlled pattern steering. The method combines mirror-image theory with transmission-optics-based phase regulation, enabling beam steering through a reconfigurable digital meta-surface that replaces the conventional ground plane. A planar dual-polarized dipole is positioned above the meta-surface, and beam steering is achieved by digitally switching the PIN-diode states to alter the discrete reflection-phase distribution. The prototype, fabricated and characterized at 12–14 GHz, demonstrates wide-angle beam steering with stable gain, low cross-polarization, and FPGA-based real-time digital control. The proposed approach provides a compact and energy-efficient solution for next-generation satellite-assisted IoT terminals requiring flexible and robust beam steering.**

***Index Terms*—beam steering antenna, meta-surface, dual-polarization**

I. Introduction

With the rapid development of electronic technology and device capabilities, the Internet of Things (IoT) has also achieved remarkable advancement. It shows significant application potential particularly in fields such as smart industrial manufacturing, healthcare, smart homes, and smart cities [1]-[4]. As one of the most promising applications in IoT, the Mobile Communication for Internet of Things (MCIoT) demonstrates significant development potential in future applications including intelligent transportation [5], low-altitude UAVs [6], and smart cities [7]. By connecting modern intelligent infrastructure such as high-speed railways trucks, and UAVs, MCIoT aims to ensure the reliability, robustness, efficiency, and convenience of information transmission for mobile intelligent devices. However, the fact that mobile entities are no longer limited to ground operations and feature high-speed movement, coupled with the limited coverage of traditional wireless communication networks, has hindered the widespread implementation of MCIoT.

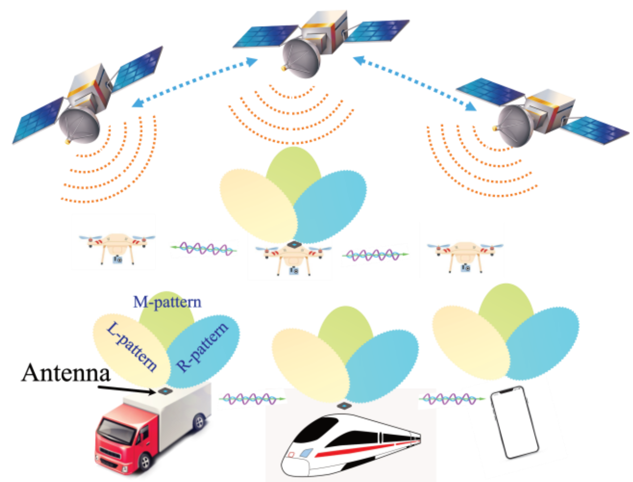

Fig. 1. Conceptual use case of the proposed beam steerable meta-surface antenna for satellite-assisted mobile communication.

Satellite-assisted MCIoT technology holds great promise as it can provide reliable and robust communication links between high-speed mobile devices and networks, especially for mobile devices such as low-altitude mobile UAVs and high-speed railways [8]. Satellite-assisted IoT enables mobile devices to communicate directly with satellites in real time, thereby enhancing accessibility. In addition, for high-altitude and sparsely populated areas, satellite communication can achieve effective coverage and reduce infrastructure deployment, thus offering a cost-effective solution for IoT.

Manuscript received Oct. xx, 2025. This work has been supported by the UK Royal Society Newton International Fellowship Alumni 2024 under Grant AL\24100018, the Natural Science Basic Research Program of Shaanxi Program under Grant 2025JC-YBMS-739, and the fundamental Research Funds for the Central Universities under No. G2024KY05102. (Corresponding author: *Guangwei Yang*)

Guangwei Yang, Gang Jiang, Yiwei Zhang, Yihan Ma, Zijian Xing, and Ling Wang are with the School of Electronics and Information, Northwestern Polytechnical University, Xi'an Shaanxi, 710129, P.R.China. (e-mail: gwyang086@gmail.com).

Lei Wang is with the with the School of Engineering, Lancaster University, LA1 4YW Lancaster, U.K. (e-mail: wanglei@ieee.org).

Dimitra Psychogiou is with the School of Engineering, University College Cork, Ireland. (E-mail: DPsychogiou@ucc.ie)

Especially, satellite-assisted MCIoT technology is advancing at a fast pace with the rapid development of reusable rocket technology.

The next generation of satellite communications (SatComs) will be delivered through a large number of Low Earth Orbit Constellations that will need to support high-capacity communication links with low latency and high data rates [9]. To facilitate these complex satellite communication scenarios, stringent requirements will need to be met by their RF transceivers, especially for the on-move IoT communication scenarios as shown in Fig. 1, which shows the future 6G-IoT integrated with Space-Air-Ground networks [10]. In these cases, beam and polarization reconfigurability, and frequency and bandwidth adaptivity will be critical to facilitate high data-rate transmission and operation in interference dominated communication environments. Conventional antennas can't meet the strident requirements for these applications due to being static, large in size, lossy or consuming high levels of DC power. As such it is really important to develop highly integrated and multifunctional antenna systems to tackle these issues.

A wide variety of reconfigurable antennas have been presented to date [11]-[15]. These include antenna architectures with reconfigurable pattern, frequency and polarization characteristics, and two or all of them. For pattern reconfigurability, alternative solutions have been presented. These include using the image theory [16], exciting multi-port or multi-mode [17]-[19], using liquid controlling technology [20], and electronic switching to changing the reflector or parasitic patches [12],[21], changing the phase constant of the parasitic strips [22], etc. Despite the large size, tuning complexity, poor radiation performance, and limited control flexibility, these tuning solutions have advanced the development of pattern reconfigurable antennas and solved many practical challenges. However, there is yet a need for technological advancements to achieve excellent pattern-reconfigurability or beam steering capability.

Meta-surface is an ultrathin two-dimensional material that can be designed to adjust the phase and amplitude of the electromagnetic wave with the aid of reconfigurable electronic components such as PIN diodes, varactors or MEMS. They have been widely used in antenna configurations for polarization conversion [23], beam steering [24], for transmitted lens [25], decoupling [26] and enhancing the antenna gain [27]. Especially, the incorporation of PIN diodes controlled by field-programmable gate array (FPGA) enables digitally tunable meta-surface structures, which lead to flexible modulation of electromagnetic waves [28].

Based on this concept, many innovative works have been investigated to realize beam steering capability [29]-[33]. In [29], a 3×3 meta-surface is employed as a parasitic layer above a patch antenna to vary the radiating pattern direction by switching the states of PIN diodes. In [30], a planar lens based on using a meta-surface was implemented to realize a steerable beam with high gain. A polarization-insensitive meta-surface unit with 2-bit phase states is used to construct a programmable reflectarray in [31], enabling dynamic beam steering by digitally controlling the states of integrated PIN diodes. [32] employs a dual-layer reflectarray architecture that enables independent beam scanning for both LHCP and RHCP, offering dual-circularly-polarized and mutually decoupled beam control. An 8×8 1-bit meta-surface based on hybrid coding mechanism is proposed in [33], which achieves active coding by switching the states of PIN diodes and introduces 2-D fixed phase delays via passive coding through unit cell rotation, realizing dual circularly polarized single-beam scanning under plane wave incidence while suppressing grating lobes. Other excellent designs using reconfigurable meta-surface technologies were presented in [34]-[37] for beam steering.

In this work, a dual-polarized pattern reconfigurable antenna using a digital meta-surface is presented for satellite-assisted MCIoT. As opposed to conventional meta-surface architectures, the proposed concept is based on a unique tuning mechanism where the meta-surfaces are used as a reconfigurable ground plane for the antenna (without increasing the antenna's profile). The phase of the reflective near-field wave is regulated flexibly. In this manner, a more accurate and flexible beam steering is achieved using a single antenna. The proposed work realizes the following unique properties: (a) a new method to realize the pattern reconfiguration; (b) dual-polarization and 2-D pattern reconfigurable capability; and (c) digital controlling pattern reconfigurable capability. The manuscript starts by presenting the pattern reconfigurable principle, followed by detailed design guidelines for the meta-surface and antenna system characteristics. Then, the manuscript presents the experimental prototype at *Ku*-band. In the end, this article is concluded.

II. Design Mechanism and Antenna Analysis

A. Pattern-controlled Mechanism

As shown in Fig. 2(a), the traditional planar dipole can radiate omnidirectionally. To increase its directivity, a metal ground can be incorporated beneath it to reflect the near-field wave. If the ground plane is placed at a distance that is one quarter of the wavelength from the dipole, a nearly directional electromagnetic radiation can be obtained. Therefore, the mirror image method can be used to solve the far-field directional pattern of the antenna. Since the mirror image of the horizontal antenna has equal amplitude and is anti-phase, the antenna can be regarded as a binary array and its array factor can be given as:

$$AF_0(\theta,\varphi) = 1 + e^{j\alpha} = 2\cos(\alpha/2) \tag{1}$$

where $\alpha = \varepsilon_0 + kd_0 cos\theta$, $\varepsilon_0 = \pi$, $d_0 = 2h_0 = \lambda/2$, k_0 is the propagation constant in free space. As such the normalized array factor can be given by (2):

$$AF_0(\theta,\varphi) = sin(\pi cos\theta/2) \tag{2}$$

Considering that the dipole antenna pattern can be given as:

$$f_0(\theta,\varphi)=\frac{\cos(\pi\sin\theta\cos\varphi/2)}{\sqrt{1-\sin^2\theta\cos^2\varphi}} \quad (3)$$

the normalized pattern of the proposed planar dipole with the metal ground can be computed using (4):

$$F_0(\theta,\varphi)=f_0(\theta,\varphi)AF_0(\theta,\varphi) = \frac{\cos(\pi\sin\theta\cos\varphi/2)}{\sqrt{1-\sin^2\theta\cos^2\varphi}}\sin(\pi\cos\theta/2) \quad (4)$$

To alter the radiation pattern characteristics, the solid ground can be replaced by the meta-surface as shown in Fig. 2(b) to change the phase of the ground. However, in this case the mirror image method listed above isn't suitable for the analysis of this configuration. Thus, a new method is presented using a combination of the mirror image and transmission optics to analyze the beam steering capabilities of the antenna with a meta-surface ground. As shown in Fig. 2(b), the incident wave is reflected at the position $P_{mn}\,(x_m, y_n, 0)$, to obtain the maximum directivity, the feeding source and its image source should direct to the same angle (θ_b, φ_b). So that they should have the same phase based on the scanning phased array principle, and is expressed as

$$\phi_{mn}+kd_{S'P}-kd_{PC}=0 \quad (5)$$

Since $d_{S'P}=d_{SP}$, so

$$\phi_{mn}=k(d_{PC}-d_{SP}) \quad (6)$$

Therefore, the source antenna and the image antenna can keep the same phase difference to direct to the same angle by the above Eq. (6). To demonstrate the proposed principle, the beam steering pointing to $(\theta_b, 0)$ at *X*-direction as an example, the phase on the meta-surface is formulated as

$$\phi_{mn}=\begin{cases}k\left(\sqrt{(x_m^2+y_n^2+h_0^2)}-h_0\cos\theta_b+y_n\sin\theta_b\right), \theta_b\neq 0\\ k\sqrt{(x_m^2+y_n^2+h_0^2)}, \theta_b=0\end{cases} \quad (7)$$

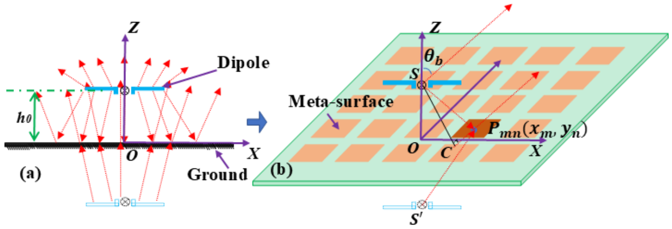

Fig. 2. Principle of operation of the proposed pattern-reconfigurable antenna: (a) Planar dipole over a conventional ground plane; (b) Planar dipole antenna over a meta-surface.

B. Meta-surface

Based on the above design principles, a meta-surface should be designed to alter the phase (ϕ_{mn}) of the reflected wave. Specifically, the design should be considered to reflect the wave at the near field, so that high-efficiency can be realized reducing the gain loss. Furthermore, the meta-surfaces will be employed in a dual-polarized antenna system. As such, the reflective polarization conversion would need to be suppressed as much as possible. Besides, active components need to be used to facilitate digital phase control in the reconfigurable reflective meta-surface.

Fig. 3 depicts the proposed meta-surface unit cell for phase reconfigurability. It is based on a four-layer metal structure with three dielectric layers. Two metal and dielectric layers (with a total thickness of only 0.6 mm) are below the ground plane and are mostly utilized for the integration of the PIN diode control circuitry, including the bias circuit network and the connectors (for connection to the FPGA module). The top layer is the radiating layer, which is a symmetrical configuration with four PIN diodes arranged around the primary radiating sheet and a metal via in the center to realize the inductance and to provide connection to ground plane. This layer is materialized on a Taconic RF-60TC substrate (with a relative dielectric constant of 6.15 and a loss tangent of 0.002, and the thickness of 1.27 mm). To facilitate DC biasing on each diode, the surrounding metal vias are linked to the controlled network on the bottom level, which are beneficial to control the diodes independently. As shown in Fig. 3(d), the bias circuitry is located between the two dielectric layers and consists of metallic routing traces and fan-shaped DC branches. Each PIN diode is connected to the bias network through a dedicated metal via, ensuring reliable DC feeding while maintaining RF isolation. The geometric parameters of the unit cell are optimized by simulation and are as follows: the period of the unit cell is 5 mm ($0.21\lambda_g$) (λg is the wavelength of the center frequency at 13GHz); Choosing a unit-cell size of approximately $\lambda_g/4$ ensures subwavelength behavior while providing sufficient resonance for effective reflection phase control, reducing phase quantization errors and maintaining stable performance under oblique incidence. L_0=3.0 mm ($0.13\lambda_g$), L_1=2.3 mm ($0.10\lambda_g$), W_0=0.4 mm ($0.02\lambda_g$), W_1=0.9 mm ($0.04\lambda_g$), W_2=0.3 mm ($0.01\lambda_g$), W_3=0.5 mm ($0.02\lambda_g$). All parameters are optimized to meet reflection amplitude and phase requirements. For example, the width W_3 controls the frequency dependence of the phase delay, and its value is chosen to ensure slow phase variation with frequency, thereby avoiding main-lobe drift, gain fluctuation, and side-lobe instability. Based on the above design, the reconfigurable reflection dual-polarization meta-surface is realized with high-efficiency and digitally adjustable capability using the PIN diodes (SMP1320-079LF). As shown in Fig. 3(b), P1 and P2 are biased to switch between 0° and 180° for the *Y*-polarization. Similarly, P3 and P4 are used to alter the phase of reflective wave on *X*-polarization. Two sets of PIN diodes enable dual polarization in the *x* and *y* directions. Since the proposed design is symmetrical, we will only analyze its performance for one of the polarizations (*X*-polarization) and the properties of the other polarization are the same.

The periodic boundary condition of the commercially-available simulation software CST Microwave Studio, is employed to investigate the capabilities of the proposed meta-surface unit cell. Low-loss PIN diodes are incorporated into each unit cell, enabling the dynamic phase manipulation of the meta-surface by switching the diode states. The equivalent RLC models of the PIN diodes in its "ON" and "OFF" states are depicted in Fig. 4. In the ON state, the diode acts as a small resistance in series with a tiny inductance, creating a low-impedance conductive path that makes the unit cell inductive and yields a reflection phase near 0°; in the OFF state, it becomes a large resistance in parallel with a junction capacitance, interrupting the current path, producing a capacitive impedance, and generating a reflection phase near 180°. Switching between these two impedance states provides a robust ~180° phase contrast and enables 1-bit programmable phase control.

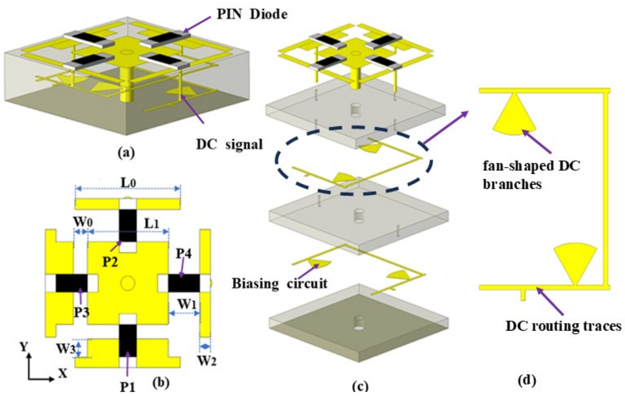

Fig. 3. Geometry of the proposed meta-surface: (a) 3D structure; (b) Plane view; (c) Expand view; (d) biasing circuitry.

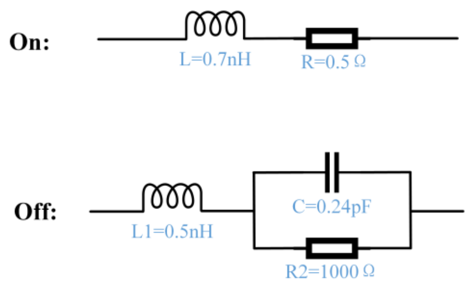

Fig. 4. Equivalent circuit model of the PIN diode when biased in its ON and OFF states.

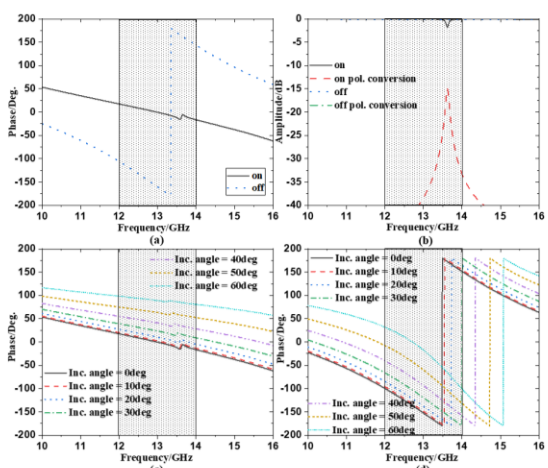

Fig. 5. Simulated reflection coefficient of the proposed meta-surface unit cell in Fig. 3 when the diodes are biased on their ON or OFF states: (a) Phase response; (b) Amplitude response; (c) Phase response for different incident angles when the diodes are ON; (d) Phase response for different incident angles when the diodes are OFF.

Based on the above design, the dual-polarization meta-surface is evaluated in terms of its reflection phase properties, which are presented in Fig. 5 (a). The design leverages PIN diodes to attain diverse reflection phase responses across the frequency range between 12 and 14 GHz. A distinct characteristic of the design is its ability to implement 1-bit coding, resulting in a phase difference of nearly 180 degrees between its two operational states (ON and OFF). When P1 and P2 are in the ON state, the reflection phase exhibits a value close to 0 degrees with a small variation of ±25°. In contrast, when both diodes are in the OFF state, the reflection phase approaches a value of 180°. The dual-polarization of the design ensures symmetrical reflection properties in both polarization states and robust performance under various operating conditions. As depicted in Fig. 5(b), the reflective amplitude remains consistently at 0 dB for *X*-polarization to *X*-polarization and *Y*-polarization to *Y*-polarization reflections, except for the frequency of 13.6 GHz in both states. Reflective cross-polarization waves exhibit values lower than -20 dB, except at 13.6 GHz. Fig. 5(c) and (d) depict the reflection phase properties of the unit cell for different oblique incident waves. As evidenced, it demonstrates stability in the phase difference between the two operational states at incidence angles up to 50°. To summarize, the proposed design facilitates the realization of a dual-polarization meta-surface with 1-bit digital phase reconfigurable capabilities while achieving good reflection coefficients.

The electric field distribution for two states is shown in Fig. 6. It reveals that, for *X*-polarization, the two strip lines on the sides of the patch produce a strong electric field when the PIN diodes are turned on. Conversely, a weak electric field is observed in Fig. 6(b) when the diodes are OFF. This pure electric field change in the design ensures efficient polarization reflection with a phase difference.

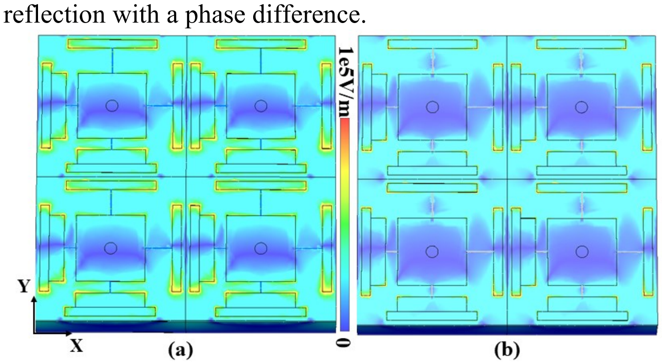

Fig. 6. Electric field distribution on the meta-surface when the diode is set: (a) On; (b) OFF.

C. *Antenna Mechanism*

The dual-polarization reflection meta-surface with 1-bit reflection phase can be used to construct a dual-polarization planar dipole antenna with beam steering based on digital control as depicted in Fig. 7. The proposed antenna system consists of a FPGA model, a 5-by-5 meta-surface array, and a dual-polarized planar dipole antenna which is fed by two coaxial cables. The meta-surface array connects to the FPGA, which outputs control signals, and the driver circuit converts them into bias voltages to control the on-off state of the PIN as a digital way. The dipole antenna is set above the meta-surface array at a height of 5 mm (the same as the height of the normal planar dipole antenna up to $0.22\lambda_g$, It can enable the reflected wave to form a favorable phase relationship with the incident wave near the array surface and reduce the profile). The parameters of the planar dipole antenna are optimized and are as follows: *Lp*=2.0 mm ($0.09\lambda_g$); *Lf*=1.8

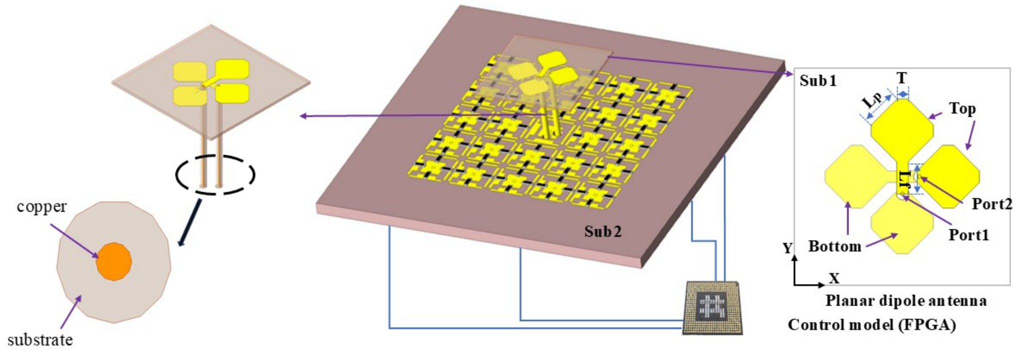

Fig. 7. Geometrical details and reconfigurability scheme of the proposed antenna configuration comprising of a dipole antenna and a reconfigurable meta-surface.

mm ($0.08\lambda_g$); and *T*=0.64 mm ($0.03\lambda_g$).

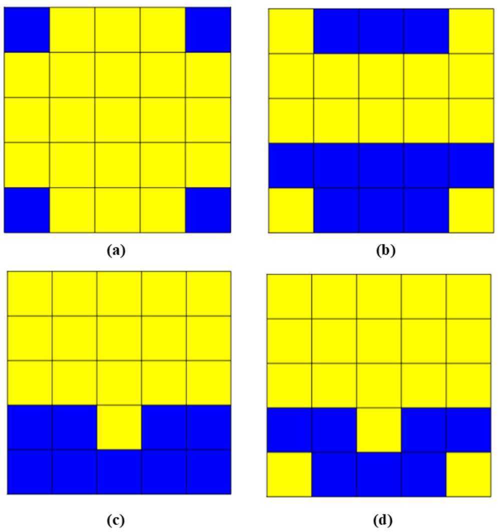

Fig. 8. Phase distribution of the reflection coefficient on meta-surface for different beam steerable states (Blue: 0°; Yellow: 180°): (a) Broadside direction; (b) 30° from broadside; (c) 45° from broadside; (d) 60° from broadside.

In Section II.A, the proposed design principle is presented. Based on the Eq. (7), the phase distribution of the plane on the meta-surface array, which should be a continuous variation and vary within -180° to 180°. Then Phase distribution is discretized due to size of the unit cell. Besides, the 1-bit phase difference is realized by the meta-surface. Hence, the appropriate value will be determined by the digital meta-surface and applied to the antenna system:

$$\varphi_{dis} = \begin{cases} 0, & -\pi/2 < \varphi_{con} < \pi/2 \\ \pi, & Otherwise \end{cases} \quad (8)$$

Where φ_{dis} is the proposed actual phase based on the proposed meta-surface. φ_{con} is the ideal phase based on the equation for every pixel on the plane. Furthermore, the phase distribution for the proposed design is shown in Fig. 8. Once the required beam steering direction and the height of the source antenna are determined, the phase distribution is obtained. In Fig. 8, the single polarization is obtained at different steerable beams. Similarly, the phase distribution of the dual-polarization can also be obtained. Therefore, the proposed technology lays a foundation for intelligent beam steering systems [38].

III. Performance Analysis and Measurements

A. Antenna Prototype and Measurement

Using as a basis the above design analysis and antenna tuning mechanism, a meta-surface antenna system was manufactured and tested in *Ku*-band to evaluate its performance. As shown in Fig. 9, a 5-by-5 dual-polarized meta-surface has been manufactured with 100 PIN diodes on the same substrate. They are connected to four PFC connectors on the bottom ground plane. These are connected to the external FPGA controller which can control every PIN diode independently. The planar dual-polarization dipole antenna is set at the meta-surface as the feeding source. In this design, each beam steering angle has a corresponding phase distribution generated by the 5-by-5 elements, so 50 outputs of independent voltages are needed to operate all the PIN diodes instantaneously and simultaneously, allowing the antenna system beam steering to be electrically scanned. Furthermore, the FPGA model provides a clock speed of 50 MHz to control the above system. As shown in Fig. 9(b), the fabricated antenna was placed in a microwave anechoic chamber for performance validation.

B. Antenna Properties

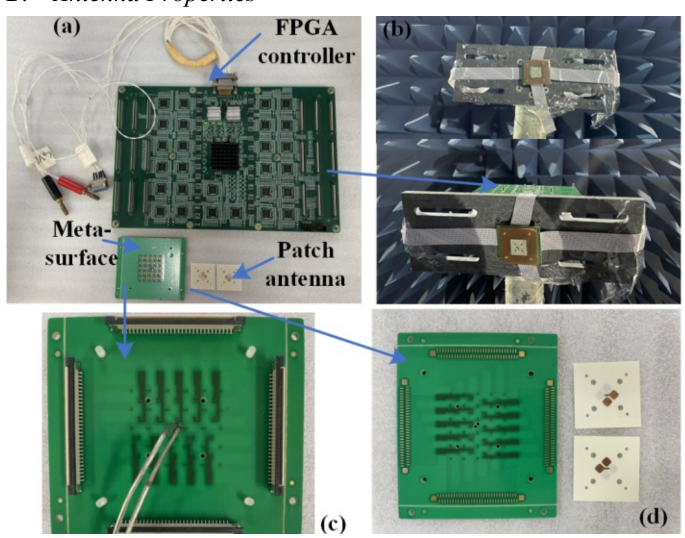

Fig. 9. Manufactured prototype of the proposed antenna system including the FPGA controller for testing: (a) All devices; (b) Experimental setup; (c) Top view of the assembled meta-surface; (d) Bottom view of the assembled meta-surface with the antenna.

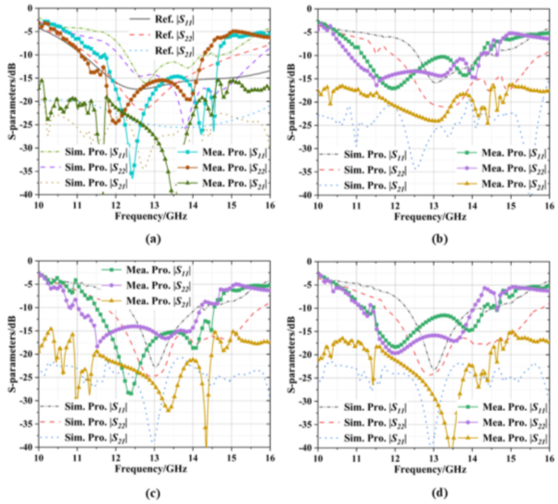

Fig. 10. Simulated and measured reflection coefficients of the proposed antenna for different beam steering states: (a) Broadside direction; (b) 30° from broadside; (c) 45° from broadside; (d) 60° from broadside.

Firstly, the *S*-parameters of the proposed antenna system are measured and shown in Fig. 10 for different biasing states. Specifically in Fig. 10(a), the simulated and measured *S*-parameters of the antenna are presented when the beam is set in broadside direction. The simulated performance of a referenced antenna with a solid ground plane is also plotted for comparison purposes. As shown, that operating bandwidth of the antenna is narrower when the meta-surface is implemented, while produces two significant resonance frequencies. Furthermore, the port isolation is slightly worse than the one of the referenced antennas but is better than 20 dB in the operating bandwidth. The *S*-parameters of the antenna for other reconfigurable states are also shown in Fig. 10. It is observed that the proposed antenna system can operate between 12 to 14 GHz and has a good port isolation (better than 20 dB) in the above frequency band. Although the simulated and measured results have some slight differences, these variations are primarily due to manufacturing and assembly errors.

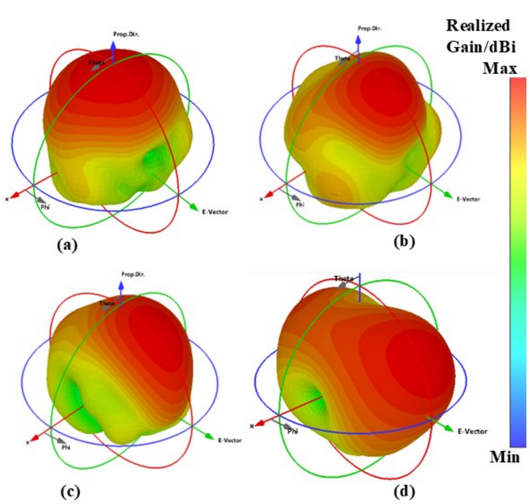

Fig. 11. 3D realized gain patterns of the proposed reconfigurable antenna for different steerable beams at 12.5 GHz: (a) broadside direction; (b) 30° from broadside; (c) 45° from broadside; (d) 60° from broadside.

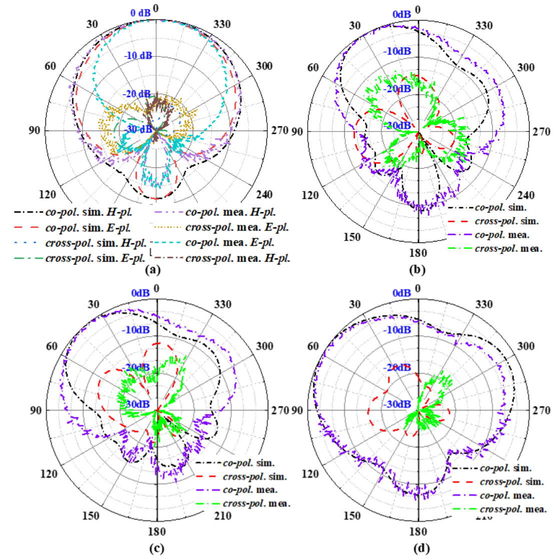

Fig. 12. Simulated and measured radiating patterns of the proposed design with different pattern-steering at 14 GHz: (a) broadside direction; (b) 30° from broadside; (c) 45° from broadside; (d) 60° from broadside.

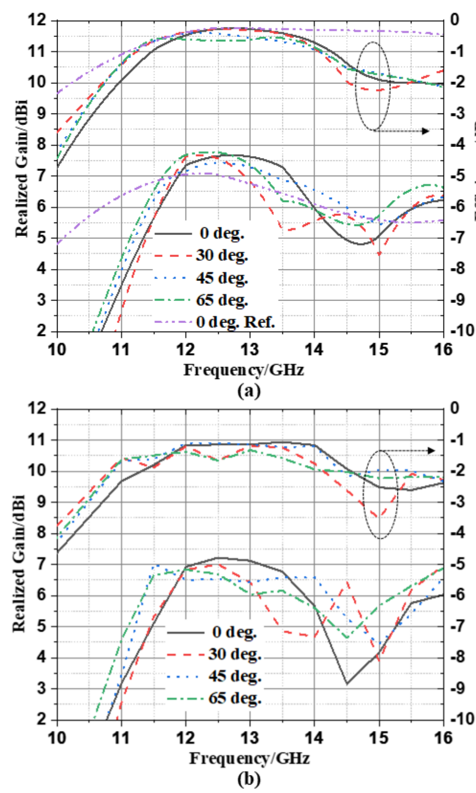

Fig. 13. Simulated and measured realized gain and efficiency of the proposed frequency band: (a) Simulation; (b) Measurement.

The 3D radiation patterns of the proposed antenna system are depicted in Fig. 11 for a frequency of 12.5 GHz and for different beam steering states are depicted in Fig. 11 to provide more intuitive views of the radiation patterns with different the beam steering. The 3D radiation patterns for the *X*-polarization can be obtained by exciting port 2. Similarly, the patterns of the *Y*-polarization can be obtained by exciting port 1. For the sake of brevity, the patterns of the *X*-polarization are used as an example to explain the proposed design. Noted that the maximum realized gains are always focused on the position at broadside direction which is a symmetric pattern since the pattern is optimized by the

TABLE I
COMPARISON OF THE WORKS

Ref.	Technology	Controlling	Size of elements/λ_g	Size of array/λ_g	Function	BW	Remark
[29]	Apertured-shared ZOR Meta-surface	electronical	0.15×0.15×0.05	0.45×0.45×0.05	Nine steerable beams	11.3%	Large range
[30]	Meta-surface lens	mechanical	0.25×0.25×1.5	30×30×10.5	2D beam steering	narrow	High gain and limited range
[31]	polarization-insensitive meta-surface	digital	0.43×0.43×0.05	5.2×5.2×0.05	Dual linear polarization	8.6%	High gain; high efficiency
[32]	Digital meta-surface	digital	0.45×0.45×0.17	7×7×0.17	Dual-Circularly Polarized Reconfiguration	4.9%	High gain; low efficiency
[33]	2-D fixed phase delays	digital	0.39×0.39×0.12	3.14×3.14×0.12	Dual Circular Polarization with Single Beam Scanning	narrow	Limited range
Pro.	**Digital meta-surface**	**digital**	**0.24×0.24×0.25**	**1.2×1.2×0.25**	**2D-pattern steering**	**15.3%**	**Dual-polarization; large range; enhancing gain**

λ_g is the wavelength of the center frequency.

meta-surface phase distribution method. Meanwhile, the beam direction of the pattern can be rotated to other directions such as $\theta = 30°, 45°, 60°$ at $\emptyset = 0°$ based on the phase distribution of the meta-surface as depicted in Fig. 11(b), (c), (d), respectively. Despite the patterns being suboptimal, the antenna is able to steer its pattern sufficiently. It is noteworthy that the performance at the large pattern steering angle is not optimal as the proposed phase distribution fails to fulfill the demands for enhanced precision control of the pattern in this regime. Nevertheless, it demonstrates the potential to steer the pattern of a single antenna.

Fig. 12 shows the simulated and measured 2D radiation patterns of the antenna system at 14 GHz for different pattern steering states. As evidenced the measured results are in general in a good agreement with the simulated ones. Specifically, in Fig. 12 (a), the broadside pattern is presented in two planes, which appears to have uniform and symmetric radiation characteristics due to the meta-surface. Furthermore, the cross-polarization is lower than -20 dB. Good radiating characteristics can also be obtained when the beam rotates to different directions using the proposed meta-surface. Although the measured patterns are affected by the presence of the active devices, the main beam of the patterns is similar to ones obtained in EM simulations. Furthermore, the simulated and measured realized gain and efficiency are reported in Fig. 13 which appear to be in a good agreement successfully validating the proposed pattern-steering concept. A comparison with the gain of the referenced antenna can be seen in Fig. 13(a). As shown, the proposed meta-surface antenna method provides a noteworthy improvement in gain of about 0.6 dB relative to the reference antenna. The efficiency of the proposed meta-surface antenna configuration for different pattern-steering states consistently remains above -1.5 dB. Furthermore, the realized gain variation of the antenna spans from 5 to 7 dBi in the proposed operating bandwidth, showcasing a robust performance across all pattern-steering scenarios.

C. *Discussion*

To highlight the proposed design advantages and novelty in relation to the state-of-art (SOA), Table I provides a detailed comparison with the SOA in beam steerable antennas. Compared with the electronically and mechanically controlled beam-scanning methods in [29] and [30], the proposed array employs digital regulation, which reduces control latency and improves the stability of phase adjustment. This enables faster and more accurate beam steering. While the designs in [29] and [31] operate with single polarization, the proposed array supports dual-polarized scanning, providing greater flexibility in practical applications and better adaptability to varying communication requirements. In terms of size, when normalized to the wavelength at the center frequency, the proposed structure is more compact than those reported in [30]–[33]. This compactness is favorable for installation and integration, particularly in space-constrained platforms. Finally, the proposed antenna achieves the widest operational bandwidth among the compared designs, offering improved frequency adaptability and more stable performance across the band.

IV. CONCLUSION

A meta-surface-based dual-polarized planar dipole antenna with the pattern-steering capability is presented for the first time in this work. The proposed antenna configuration uses basis a novel tuning mechanism where a reconfigurable meta-surface ground plane formed by 5×5 phase-reconfigurable unit cells is incorporated beneath the dipole to reconfigure the direction of the radiation pattern. The proposed antenna system was designed, manufactured and measured to verify the proposed pattern-steering approach. It is demonstrated that the proposed meta-surface tuned dipole antenna can operate between 12 to 14 GHz and is able to reconfigure its beam from 0° to 60° with high gain between 5-7 dBi and efficiency of more than -2 dB. Therefore, this design would be a promising candidate for satellite-assisted mobile communications because of its flexible and excellent beam-steering capability.

REFERENCES

[1] E. H. Houssein, M. A. Othman, W. M. Mohamed and M. Younan, "Internet of Things in Smart Cities: Comprehensive Review, Open Issues, and Challenges," *IEEE Internet of Things Journal*, vol. 11, no. 21, pp. 34941-34952, 1 Nov.1, 2024.

[2] D. C. Nguyen, "6G Internet of Things: A comprehensive survey," *IEEE Internet Things J.*, vol. 9, no. 1, pp. 359–383, Jan. 2022.

[3] Y. You, Y. Lu, J. Xu and J. Huang, "High Gain Monopulse Variable Inclination Continuous Transverse Stub Antenna for Satellite-Aided Vehicular Communications," *IEEE Internet of Things Journal*, vol. 9, no. 23, pp. 24346-24356, 1 Dec.1, 2022.

[4] T. R. Wanasinghe, R. G. Gosine, L. A. James, G. K. I. Mann, O. de Silva, and P. J. Warrian, "The Internet of Things in the oil and gas industry: A systematic review," *IEEE Internet Things J.*, vol. 7, no. 9, pp. 8654–8673, Sep. 2020.

[5] Z. Wang, S. Han and Y. Dong, "Miniaturized Quad-Polarized Pattern Reconfigurable Antenna for Intelligent IoT Applications," *IEEE Internet of Things Journal*, vol. 11, no. 21, pp. 35361-35375, 1 Nov.1, 2024.

[6] D. -T. Do, C. -B. Le, A. Vahid and S. Mumtaz, "Antenna Selection and Device Grouping for Spectrum-Efficient UAV-Assisted IoT Systems," *IEEE Internet of Things Journal*, vol. 10, no. 9, pp. 8014-8030, 1 May1, 2023.

[7] Z. Xing *et al*., "Dual-Band Quad-Polarized Anti-Multipath Interference Antenna for IoT Indoor Backscatter Positioning," *IEEE Internet of Things Journal*, vol. 12, no. 20, pp. 43707-43719, 15 Oct.15, 2025.

[8] R. Alwahishi, M. M. M. Ali, G. H. Elzwawi, and T. A. Denidni, "Beam-switching antenna using reconfigurable intelligent frequency selective surfaces for Internet of Things applications," *IEEE Internet Things J.*, vol. 11, no. 3, pp. 4152–4162, Feb. 2024.

[9] O. Kodheli, E. Lagunas, N. Maturo, S. K. Sharma, et al., "Satellite Communications in the New Space Era: A Survey and Future Challenges," *IEEE Communications Surveys & Tutorials*, vol. 23, no. 1, pp. 70-109, First quarter 2021.

[10] T. Lou, X. -X. Yang, G. Tan and S. Gao, "Shared Aperture Dual-Band Dual Circularly Polarized Multibeam Antenna for Satellite-Assisted Internet of Vehicles," *IEEE Internet of Things Journal*, vol. 11, no. 7, pp. 12000-12011, 1 April, 2024.

[11] L. Santamaria, F. Ferrero, R. Staraj and L. Lizzi, "Slot-Based Pattern Reconfigurable ESPAR Antenna for IoT Applications," *IEEE Trans. Antennas Propag.*, vol. 69, no. 7, pp. 3635-3644, July 2021.

[12] G. Yang, J. Li, D. Wei, S. Zhou and R. Xu, "Pattern Reconfigurable Microstrip Antenna with Multidirectional Beam for Wireless Communication," *IEEE Trans. Antennas Propag.*, vol. 67, no. 3, pp. 1910-1915, March 2019.

[13] Q. Chen, J. Li, G. Yang, B. Cao and Z. Zhang, "A Polarization-Reconfigurable High-Gain Microstrip Antenna," *IEEE Trans. Antennas Propag.*, vol. 67, no. 5, pp. 3461-3466, May 2019.

[14] G. Yang, J. Li, B. Cao, D. Wei, S. Zhou and J. Deng, "A Compact Reconfigurable Microstrip Antenna with Multidirectional Beam and Multipolarization," *IEEE Trans. Antenna Propag.*, vol. 67, no. 2, pp. 1358-1363, Feb. 2019.

[15] Jun Hu, Zhang-Cheng Hao, "A Compact Polarization-Reconfigurable and 2-D Beam-Switchable Antenna Using the Spatial Phase Shift Technique," *IEEE Trans. Antennas Propag.*, vol. 66, no. 10, pp. 4986-4995, Oct. 2018.

[16] G. Yang, R. Adil, Y. Zhang, Z. Xing, Z. Chen, Q. Luo and Y. Ma, "Preparation of Linear Array Antenna for 2D-Scanning Capability Based on the Generalized Phase Array Theory," *IEEE Transactions on Antennas and Propagation*, Early Access, doi: 10.1109/TAP.2025.3645937.

[17] Z. Zhu, S. Zheng, X. Xiong, Y. Chen, et al., "A Compact Pattern Reconfiguration Antenna Based on Multimode Plane Spiral OA," *IEEE Trans. Antennas Propag.*, vol. 69, no. 2, pp. 1168-1172, Feb. 2021.

[18] C. Sulakshana, K. Dahal and L. Anjaneyulu, "Pattern reconfigurable antenna with multi-port excitation for K-band application," 2017 IEEE International Conference on Microwaves, Antennas, Communications and Electronic Systems (COMCAS), 2017, pp. 1-5.

[19] J. You and Y. Dong, "Pattern-Reconfigurable Dipole Antenna Based on Odd- and Even-Mode Principle for 5G-NR Communications," *IEEE Transactions on Antennas and Propagation*, vol. 72, no. 10, pp. 8028-8033, Oct. 2024.

[20] X. Yang, Y. Liu, H. Lei, Y. Jia, P. Zhu, and Z. Zhou, "A radiation pattern reconfigurable Fabry–Pérot antenna based on liquid metal," *IEEE Trans. Antennas Propag.,* vol. 68, no. 11, pp. 7658–7663, Nov. 2020.

[21] Y. Zhang, S. Tang, J. Rao, C. -Y. Chiu, X. Chen and R. Murch, "A Dual-Port Dual-Beam Pattern-Reconfigurable Antenna With Independent 2-D Beam-Scanning," *IEEE Transactions on Antennas and Propagation*, vol. 72, no. 10, pp. 7628-7643, Oct. 2024.

[22] J. Lu, H. C. Zhang, P. H. He, M. Wang and T. J. Cui, "Pattern Reconfigurable Yagi Antenna Based on Active Corrugated Stripline," *IEEE Transactions on Antennas and Propagation*, vol. 71, no. 1, pp. 1011-1016, Jan. 2023.

[23] K. -Y. Liu, G. -M. Wang, T. Cai, H. -P. Li and T. -Y. Li, "Conformal Polarization Conversion Metasurface for Omni-Directional Circular Polarization Antenna Application," *IEEE Trans. Antenna Propag.*, vol. 69, no. 6, pp. 3349-3358, June 2021.

[24] G. Yang and S. Zhang, "Dual-Band Shared-Aperture Multiple Antenna System with Beam Steering for 5G Applications," IEEE Transactions on Circuits and Systems II: Express Briefs, vol. 69, no. 12, pp. 4804-4808, Dec. 2022.

[25] Li-Zhao Song, Yun-Ze Diao, Pei-Yuan Qin, Maral Ansari, Jeff von Loesecke, Stefano Maci, Y. Jay Guo, "A 3-D-Printed Broadband Wide-Angle Multibeam Flat GRIN Lens Aided by Multifocal Ray-Path Analyses", *IEEE Trans. Antenna Propag.*, vol.73, no.1, pp.22-32, 2025.

[26] S. Luo, Y. Zhang, G. F. Pedersen and S. Zhang, "Mutual Decoupling for Massive MIMO Antenna Arrays by Using Triple-Layer Meta-Surface," IEEE Open Journal of Antennas and Propagation, vol. 3, pp. 1079-1089, 2022.

[27] K. E. Kedze, H. Wang and I. Park, "A Metasurface-Based Wide-Bandwidth and High-Gain Circularly Polarized Patch Antenna," *IEEE Trans. Antenna Propag.*, vol. 70, no. 1, pp. 732-737, Jan. 2022.

[28] T. J. Cui, M. Q. Qi, X. Wan, J. Zhao, Q. Cheng, "Coding metamaterials, digital metamaterials and programmable metamaterials," *Light. Sci. Appl.* vol. 3, no. 10, e218, Oct. 2014.

[29] Z. Wang, S. Zhao and Y. Dong, "Pattern Reconfigurable, Low-Profile, Vertically Polarized, ZOR-Metasurface Antenna for 5G Application," *IEEE Trans. Antenna Propag.*, vol. 70, no. 8, pp. 6581-6591, Aug. 2022.

[30] Francesco Alessio Dicandia, Simone Genovesi, "Mechanically Steerable Simultaneous Multibeam Transmitarray Design by Analytical Multifocal Approach", *IEEE Trans. Antenna Propag.*, vol.72, no.12, pp.9129-9142, 2024.

[31] N. Yang *et al.*, "A 2-Bit Programmable Reflectarray Antenna Based on a Polarization-Insensitive Metasurface," *IEEE Trans. Antennas Propagat.*, vol. 72, no. 7, pp. 5539–5549, July 2024.

[32] S. Zhou, F. Yang, S. Xu, and M. Li, "A Dual-Circularly Polarized Reconfigurable Reflectarray Antenna With Independent Beam Scanning Capability," *IEEE Trans. Antennas Propagat.*, vol. 72, no. 9, pp. 7100–7109, Sept. 2024.

[33] W. Li, X. Wang, Y. Wang, N. Yan, G.-M. Yang, and Y.-Q. Jin, "Single-Beam-Scanning 1-bit Metasurface With Dual Circular Polarization Based on Hybrid Coding Mechanism," *IEEE Trans. Antennas Propagat.*, vol. 73, no. 3, pp. 1608–1617, Mar. 2025.

[34] R. Y. Wu, L. Zhang, L. Bao, L. W. Wu, Q. Ma, G. D. Bai, *et al*. "Digital metasurface with phase code and reflection–transmission amplitude code for flexible full-space electromagnetic manipulations," Advanced Optical Materials, vol. 7, no. 8, 1801429, Apr. 2019.

[35] H. Rajabalipanah and A. Abdolali, "Ultrabroadband Monostatic/Bistatic RCS Reduction via High-Entropy Phase-Encoded Polarization Conversion Metasurfaces," IEEE Antennas and Wireless Propagation Letters, vol. 18, no. 6, pp. 1233-1237, June 2019.

[36] X. G. Zhang, W. X. Jiang, H. L. Jiang, *et al*. "An optically driven digital metasurface for programming electromagnetic functions," *Nat Electron* vol. 3, pp. 165–171, Mar. 2020.

[37] F. Wu, R. Lu, J. Wang, Z. H. Jiang, W. Hong and K. -M. Luk, "A Circularly Polarized 1 Bit Electronically Reconfigurable Reflectarray Based on Electromagnetic Element Rotation," *IEEE Trans. Antenna Propag.*, vol. 69, no. 9, pp. 5585-5595, Sept. 2021.

[38] Y. Ma, Y. Guo, Q. Luo, Y. Zhou, G. Yang and S. Gao, "Phase-Only Pattern Synthesis of Domino Tiling Irregular Arrays Based on Deep Reinforcement Learning and Gradient-Descent Optimization," *IEEE Transactions on Antennas and Propagation*, vol. 73, no. 8, pp. 5623-5636, Aug. 2025.

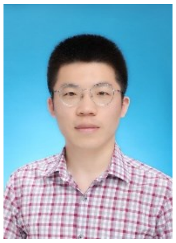

Guangwei Yang (S'15-M'19-SM'23) received the B.E., M.S., and Ph.D. degrees in electronic engineering from Northwestern Polytechnical University (NPU), Xi'an, China, in 2012, 2015, and 2019, respectively. He is currently a Professor of electronic engineering with NPU and Newton International Fellow of Royal Society, U.K. Prior to joining NPU, he was a Senior Researcher at Tyndall National Institute, Cork, Ireland; and a Research Fellow at Queen Mary University of London, London, U.K.; and held a post-doctoral position at the Antenna, Propagation and Millimeter wave Systems (APMS) Section, Aalborg University, Aalborg, Denmark. His recent research interests include AI for beamforming, THz technology, microstrip antennas, wideband antennas, millimeter-wave array antennas, circularly polarized antennas, phased array antennas and theory, reconfigurable antennas, scanning antennas, wireless communication, and metasurfaces. He has been an Elected Member of the Board of Directors of Microwave Branch of the Chinese Institute of Electronics since 2025. Dr. Yang serves as a reviewer for all the IEEE and IET journals related to antennas, a Top Reviewer for IEEE Transactions on Antennas and Propagation (TAP), and an Outstanding Reviewer for IEEE Antennas and Wireless Propagation Letters (AWPL). He was also a guest lead editor and co-editor of two special issues on scanning antenna and metasurfaces and a Lead Guest Editor for the Special Cluster on Emerging Beam Steering Technologies of Antenna Systems of IEEE ANTENNAS AND WIRELESS PROPAGATION LETTERS in 2025.

Gang Jiang received the B.S. degree in Electronic and Information Engineering from Xidian University, Xi'an, China, in 2011, and the M.S. degree in Electronics and Communication Engineering from the same university in 2014. He is currently pursuing the Ph.D. degree in New Generation Electronic and Information Engineering at Northwestern Polytechnical University, Xi'an, China.

Since 2014, he has been serving as a Senior Engineer at the 20th Research Institute of China Electronics Technology Group Corporation (CETC). His research interests include antenna and microwave radio frequency, radar system integration, and electronic countermeasures. He has participated in and presided over a number of national-level pre-research and scientific research projects, and has published numerous related papers and patents.

Yiwei Zhang received the B.E. degree in communication engineering from Shandong University, Qingdao, China, in 2024. He is currently pursuing the M.E. degree at Northwestern Polytechnical University, Xi'an, China. His research interests include millimeter-wave wide-angle scanning antennas and metasurface antennas.

Yihan Ma received the bachelor's and master's degrees from the School of Electronics and Information, Northwestern Polytechnical University, Xi'an, China, in 2014 and 2017, respectively, and the Ph.D. degree from the School of Electronic Engineering and Computer Science, Queen Mary University of London, London, U.K.

He is currently a Research Associate with the University of Hertfordshire. His research interests include the phased array antennas and theory, metasurface design, and machine learning.

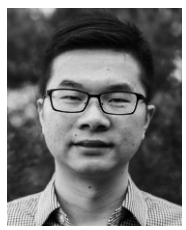

Lei Wang (Senior Member, IEEE) received the Ph.D. degree in electromagnetic field and microwave technology from the Southeast University, Nanjing, China, in 2015.,From 2014 to 2016, he was a Research Fellow with the Swiss Federal Institute of Technology (EPFL), Lausanne, Switzerland. From 2016 to 2017, he was a Post-Doctoral Researcher with the KTH Royal Institute of Technology, Stockholm, Sweden. From 2017 to 2020, he was an Alexander von Humboldt Fellow with Hamburg University of Technology, Hamburg, Germany. From 2020 to 2023, he was an Assistant Professor with the Heriot-Watt University, Edinburgh, U.K. Since 2024, he has been an Associate Professor (Senior Lecturer) with Lancaster University, Lancaster, U.K. He has published more than 100 peer-review papers, book chapters, in addition to U.K. and U.S. patents. His research includes antenna theory and applications, active electronically scanning arrays, integrated antennas and arrays, substrate-integrated waveguide antennas, leaky wave antennas, wireless power transfer, and wireless propagations. Dr. Wang was a recipient of the National Ph.D. Scholarship from China in 2014, the Swiss Government Excellence Scholarship in 2014, the Alexander von Humboldt Fellowship in 2016, the Principal Investigator Grant from German Research Foundation (DFG) in 2020, the British Royal Society Research Grant in 2022, U.K. EPSRC International Collaboration Grant in 2023, the Innovate U.K. Grants in 2024 and 2025, and the Sony Research Award in 2025. Moreover, he also received the Best Poster Award from iWAT in 2018, the Best Paper Award from UCET in 2020, and the Best Antenna Paper Award from EuCAP in 2023. He also supervised students winning the Honorable Mentioned Best Student Paper Award from APS in 2021, the Best Student Paper Award from UCMMT in 2022, and the Second Place Winner from IWS in 2023.

Zi-Jian Xing received the B.E., M.E., and Ph.D. degrees from Northwestern Polytechnical University, Xi'an, China, in 2008, 2011, and 2014, respectively.

In 2014, he worked as an Assistant Professor with Northwestern Polytechnical University, where he became an Associate Professor in July 2018. He has published over 20 research journal articles in IEEE and many international conferences. He is a reviewer of all the IEEE journals related to antennas. He has researched and designed a variety of navigation antenna arrays, stealth antenna radome, and radio frequency identification antennas. His research interests include circularly polarized antenna arrays, reconfigurable antenna, stealth antennas, and near-field antenna technology.

Dimitra Psychogiou (Senior Member, IEEE) received the Dipl.-Eng. degree in electrical and computer engineering from the University of Patras, Patras, Greece, in 2008, and the Ph.D. degree in electrical engineering from Swiss Federal Institute of Technology (ETH), Zürich, Switzerland, in 2013.,She was a Senior Research Scientist with Purdue University, West Lafayette, IN, USA, and an Assistant Professor with the University of Colorado at Boulder, Boulder, CO, USA. She is currently a Professor of electrical and electronic engineering with the University College Cork (UCC), Cork, Ireland; the Head of the Advanced RF Technology Group, Tyndall National Institute, Cork; and also a Research Professor. Her research has been presented in more than 200 IEEE publications. Her current research interests include RF design and characterization of reconfigurable microwave and millimeter-wave passive components and antennas, RF MEMS, acoustic wave resonator-based filters, tunable filter synthesis, and additive manufacturing techniques for 3-D antenna systems. Dr. Psychogiou is a Senior Member of URSI and a member of the IEEE MTT-S Filters and Passive Components (MTT-5) and the Microwave Control Materials and Devices (MTT-13) Committees. Furthermore, she serves on the Technical Review Board for various IEEE and EuMA conferences and journals. She received the 2021 Research Professorship Award from the Research Ireland, the 2021 Roberto Sorrentino Prize from European Microwave Association (EuMA), the 2020 CAREER Award from the National Science Foundation (NSF), USA, the 2020 URSI Young Scientist Award, and the Junior Faculty Outstanding Research Award from UC Boulder. She serves as the Chair for MMT-13 and the Secretary for the USNCURSI Commission D. She was an Associate Editor of IET Microwaves, Antennas and Propagation. She is also an Associate Editor of IEEE Microwave and Wireless Components Letters and International Journal of Microwave and Wireless Technologies.

Ling Wang (Member, IEEE) received the B.Sc., M.Sc., and Ph.D. degrees in electronic engineering from Xidian University, Xi'an, China, in 1999, 2002, and 2004, respectively. From 2004 to 2007, he was with Siemens, Munich, Germany, and Nokia Siemens Networks, Espoo, Finland. Since 2007, he has been with the School of Electronic and Information, Northwestern Polytechnical University, Xi'an, where he became a Professor in 2012. His current research interests include array processing and smart antennas, wideband communications, cognitive radio, adaptive antijamming for satellite communications, satellite navigation, and data link systems.